



Robot Control Algorithms Based on Sclera Force Information

Ali Ebrahimi, group 7

Mentors: Dr. Marin Kobilarov, Dr. Iulian Iordachita, Dr. Russell H. Taylor and Dr. Nirav Patel

May 11th, 2018

Computer Integrated Surgery II

Dr. Russell H. Taylor

Spring 2018

Johns Hopkins University, Baltimore, MD

Table of Contents

| | | |
|-------|---|----|
| 1 | Introduction..... | 3 |
| 1.1 | Summary | 3 |
| 1.2 | Specific goals..... | 4 |
| 1.3 | Significance | 4 |
| 2 | Background and Material..... | 4 |
| 2.1 | Steady Hand Eye-robot (SHER) | 5 |
| 2.2 | Dual force-sensing tool | 6 |
| 2.3 | Eye phantom | 7 |
| 3 | Technical approach | 7 |
| 3.1 | Piezo-actuated linear stage | 8 |
| 3.2 | Obtaining standards for surgeon’s behavior | 9 |
| 3.3 | Control approaches..... | 10 |
| 3.3.1 | The first variable admittance control | 10 |
| 3.3.2 | The second variable admittance control | 12 |
| 3.3.3 | Auditory feedback | 14 |
| 3.4 | Conclusion..... | 14 |
| 4 | Results | 14 |
| 4.1 | Pilot studies (for the first and third control)..... | 15 |
| 4.2 | Results of the SIMULINK simulations for the second control method | 16 |
| 4.3 | Multi-user experiment | 18 |
| 5 | Conclusion | 19 |
| 6 | Challenges and Issues..... | 20 |
| 7 | Management Plan, Reading List and References..... | 20 |
| 8 | Deliverables and Milestones | 20 |
| 9 | Acknowledgements | 21 |
| 10 | References | 21 |

1 Introduction

1.1 Summary

One of the major yet little recognized challenges in robotic vitreoretinal surgery (Figure 1) is the matter of tool forces applied to the sclera (Figure 2). Tissue safety, coordinated tool use and interactions between tool tip and shaft forces are little studied. The introduction of robotic assist has further diminished the surgeon's ability to perceive scleral forces. Microsurgical tools capable of measuring such small forces integrated with robot-manipulators may therefore improve functionality and safety by providing sclera force feedback to the surgeon. In this project, first we are going to develop two different standards for safe and adept eye manipulation based on an expert behavior. Then, using a force-sensing tool (Figure 3), we are going to implement two control algorithms on Eye-robot 2.1 (Figure 4) to provide the surgeon with haptic force feedback based on the developed standards to escalate the sclera safety and reduce the detrimental forces during eye manipulation. In addition to the haptic feedback, we are going to provide the subjects with auditory feedback which informs them about the level of sclera force they are applying.



Figure 1: The vitreo-retinal surgery

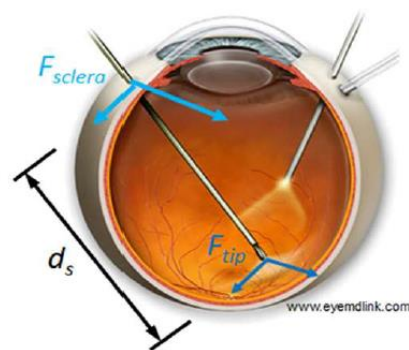


Figure 2: Different forces on the eye-ball

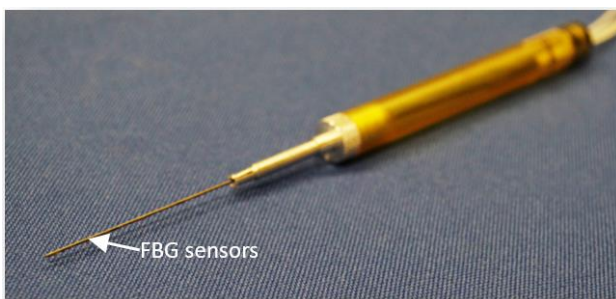


Figure 3: force-sensing tool

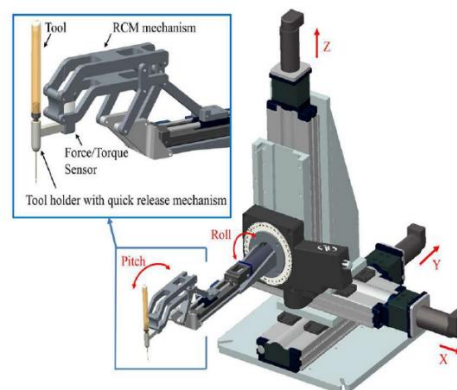


Figure 4: Eye-robot 2.1

1.2 Specific goals

The specific goals of the project are encapsulated in the bullet points below:

- Preparing the experimental setup including the (Eye-robot 2.1, force-sensing tools, eye-phantom) and ensuring that all the system components work properly and we are receiving correct force data.
- Obtaining two kinds of safety standard based on the expert's surgeon behavior
- Developing two different variable admittance robot control laws (an adaptive and a non-adaptive one) to increase the sclera safety
- Each control algorithm should be appropriate to its corresponding safety standard
- Providing audio feedback to the subjects to inform the unsafe levels of sclera force
- Assembling and programming a piezo-actuated linear stage to simulate the movement of the eyeball during the surgery
- Conducting pilot studies to see how the system functionality
- Conducting multi-user experiments within the Homewood campus with 10 different users
- Analyzing the results to see how the haptic feedback and the auditory feedback may help reducing the sclera force level

1.3 Significance

To the best of the author's knowledge audio feedback was derived only from the tool tip force only in the prior studies in this area [4]. However, the sclera force becomes more impactful than the tip force as the surgical tool is always in contact with the sclera, while tool tip has intermittent contact with the retina. Thus, providing real-time sclera force feedback could potentially improve the scleral tissue safety. The focus of this study is therefore to provide subjects with various types of sclera force feedback including haptic and auditory in order to assess their influence on sclera safety. We hypothesize that providing either passive or active (audio or haptic) feedback may help limit forces that exceed a predefined safety threshold. Again, To the best of our knowledge, it is the first time that either haptic or auditory feedback for sclera force is being provided during eye manipulation which is accomplished by modifying the control algorithm of the SHER. Finally, the results are compared to find out the efficiency of providing feedback.

2 Background and Material

Vitreoretinal surgery continues to be one of the most challenging surgical procedures as it requires micron scale tool manipulations and delicate tissue interactions in which physiological hand tremor may degrade the performance during the surgery. Over the last two decades, several kinds of robotic systems including Master-Slave and Cooperatively controlled robots have

been deployed to either eliminate or diminish the hand tremor to provide more accurate surgical tool positioning. The robotics assistance could definitely provide precise tool motion; however, the dominant stiffness and inertia of the robot prevents the surgeon from perceiving very small scleral forces (resulting from contact between the surgical tool shaft and the sclera). This diminishes the surgeon's ability to bimanually manipulate the eye and puts the sclera at risk for injury. Therefore, the focus of this project is to increase sclera force safety by implementing different control algorithms on the Steady Hand Eye-robot 2.1 and also providing auditory feedback using the online sclera force data.

The two pivotal components of this project which have been developed recently by other researchers at JHU are 1- the Steady Hand Eye-Robot (SHER) 2- Force-sensing tool. The general picture of the prepared experimental setup is depicted in Figure 5.

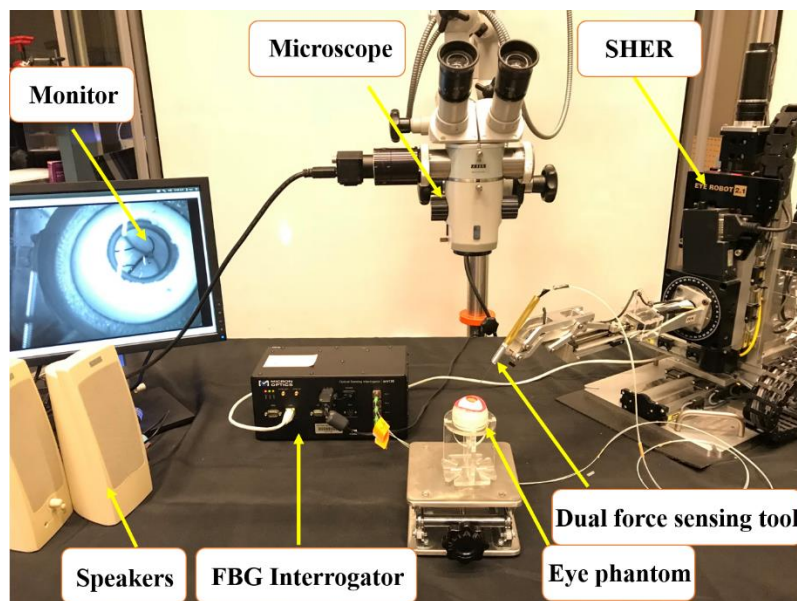


Figure 5: Experimental setup: The steady-Hand Eye Robot, ZEIS Microscope, FBG Interrogator, Eye phantom, Dual force-sensing tool

2.1 Steady Hand Eye-robot (SHER)

The Steady-Hand Eye Robot (SHER) shown in Figure 4 is a cooperatively controlled robot that is intended to reduce hand tremor and has been developed at Johns Hopkins University [1]. Both the surgeon and the robot simultaneously hold the tool, and by a proportional impedance control enforced by the robot the operator performs a steady and tremor-free manipulation. The robot's generic impedance control scheme sets the end-effector velocity to be proportional to operator's contact force F_h (the interaction force between robot end-effector and operator's hand which is measured by a 6 DOF force sensor attached to the end-effector). This general control scheme is

shown in Eq. (1). Our purpose in this project is to modify this control law to achieve the safety goals discussed above.

$$\dot{x}_d = \Lambda F_h \quad (1)$$

2.2 Dual force-sensing tool

The theory for this force-sensing tool was previously developed by [2]. As represented in Figure 6, 3 optical FBG strain sensors are attached around the perimeter of a 25-gauge nitinol needle. As explained in [2], by finding the related calibration matrices for this configuration of FBG sensors, we would be able to relate the raw optical wavelength data of FBGs to the sclera force (F_s), tool tip force (F_t) and insertion depth (the length of the tool inside the eye). The FBG fibers are connected to an optical sensing interrogator (sm130-700 from Micron Optics Inc., Atlanta, GA) which sends the FBG raw data with maximum frequency of 1 KH to the computer to calculate real-time force data (Figure 5).

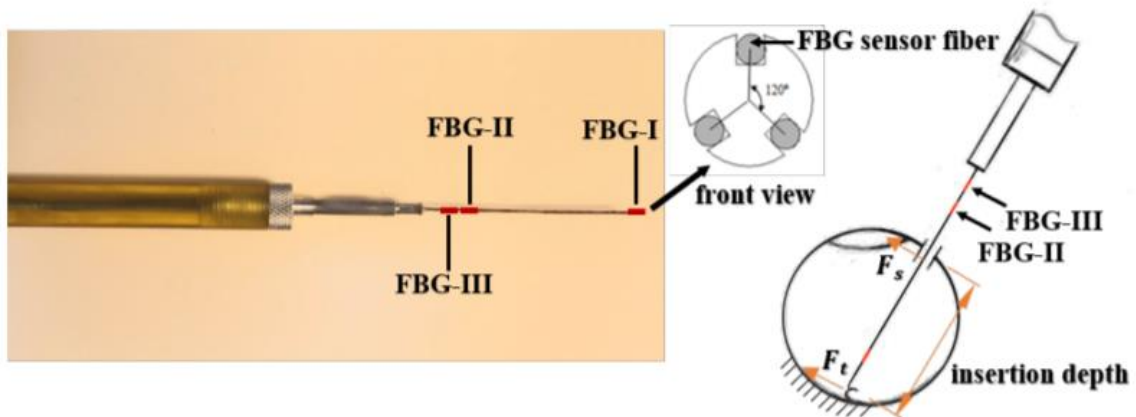


Figure 6: Dual force-sensing tool and the interaction forces of the tool with the eyeball

After calibrating the tool, we performed validation experiments to evaluate the accuracy of the calculated sclera force and insertion depth. By using the tool as a cantilever beam, 50 known sclera forces at known insertion depths were applied to the tool shaft and the force values were recorded by a very precise scale (Sartorius ED224S Extend Analytical Balance, Goettingen Germany). Then, the sclera force and insertion depth for those points were calculated using the calibration matrices. Fig. 3 depicts the calculated and real values for sclera force and insertion depth. The RSME for sclera force and insertion depth validation experiments are 1.2 mN and 0.5 mm, respectively (calculated with MATLAB). Figure 7 represents the validation results for the tool.

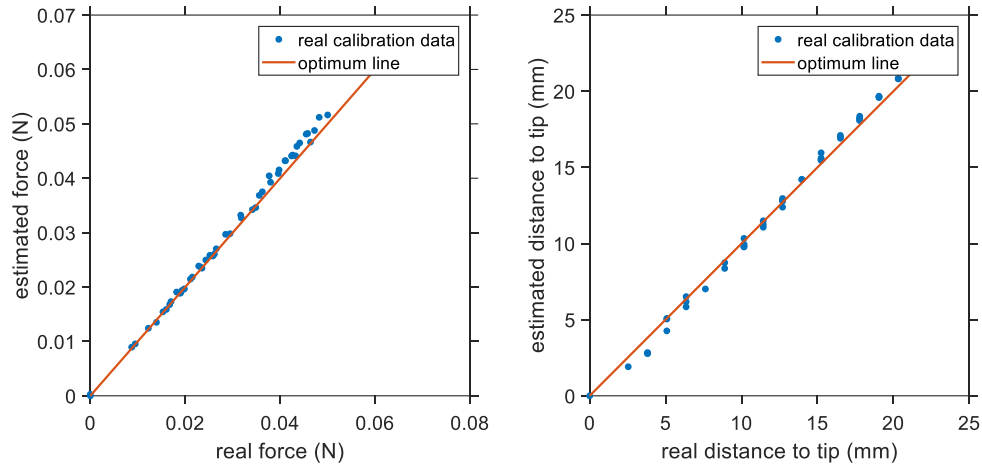


Figure 7: Validation results for the dual-tool calibration

2.3 Eye phantom

The artificial eye phantom is made from Silicon. It is placed into a 3D-printed socket lubricated with mineral oil to produce realistic friction coefficient between the eye phantom and the socket. Also, to create an environment similar to a real eye surgery, we have utilized a ZEISS microscope to observe inside the eyeball during the experiments. A Point Grey camera (FLIR Systems, Inc.) is attached to the microscope for recording the user interaction with the eyeball. In addition, as shown in colored vessels printed on a paper are attached into the eyeball.

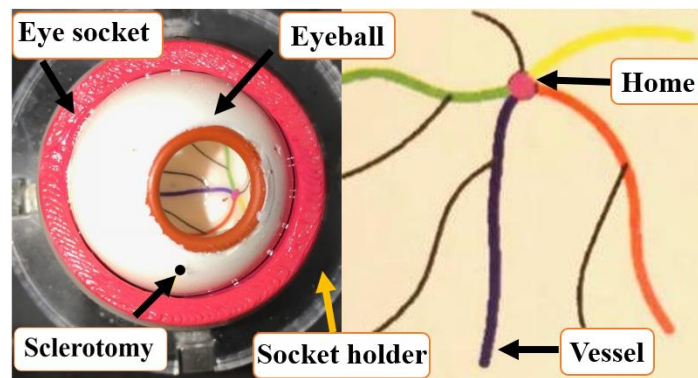


Figure 8: Eye phantom with outer diameter of 30 mm

3 Technical approach

In this part the process of accomplishing different goals of the project is elaborated. As discussed before, to simulate the behavior of the eye during the surgery we have utilized a 3D linear stage. This linear stage is explained in details in part **Error! Reference source not found.** . T

hen, in part 3.2 the procedure in which we obtained the surgeon's behavior is delineated. Finally, in part 3.2 the control approaches and the provided audio feedbacks are elaborated.

3.1 Piezo-actuated linear stage

The linear stage used here is from PI Q-motion Stages with controller number of E-873.3QTU. It is a very sensitive and fragile piezo-actuated stage that is able to move in 3 perpendicular directions with amplitude of 6 mm. First off, we assembled the stage by the instructions given by PI. After preparing the stage, we designed an eye socket which is able to be attached to the stage. For designing the eye socket, we should have taken into account the weight of the stage because there were 1 N restrictions on the vertical force exerted on the stage. After 3D printing the eye-socket, we put the eye phantom inside the eye socket. The final picture of the assembled stage and the eye socket is depicted in Figure 9.

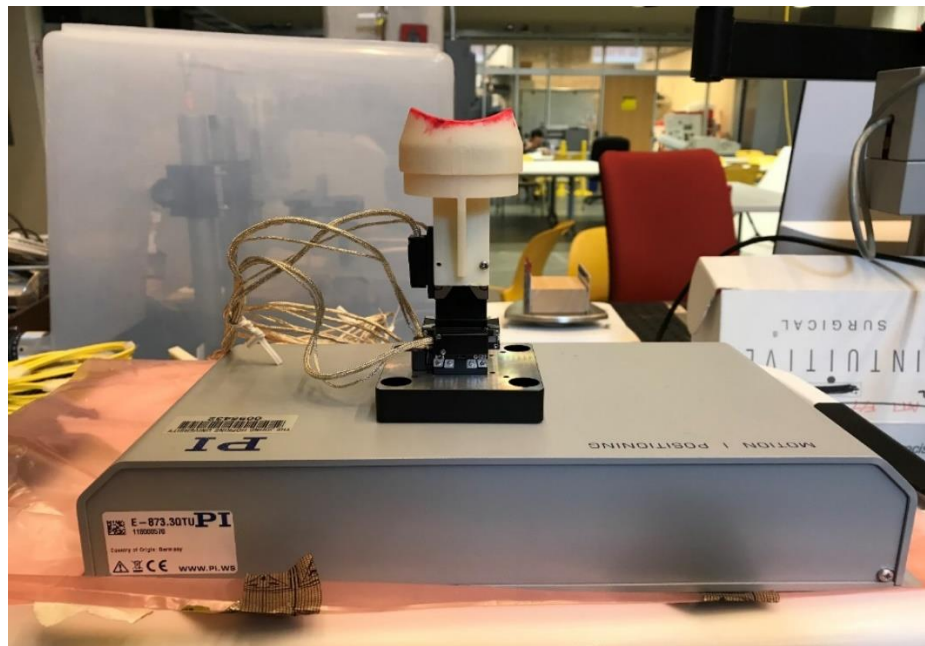


Figure 9: Eye phantom attached to the piezo-actuated linear stage

After assembling the stage, we started programming the stage using the MATLAB driver provided by the producer company. After installing the MATLAB driver, we could access to the several classes which facilitated programming the stage movement and manipulating the data transferred between the computer and the stage controller. Finally, we decided to produce a horizontal movement with amplitude of 1 mm with period of 1.5 s as the simulator of the eye movement in the horizontal direction.

3.2 Obtaining standards for surgeon's behavior

- The first curve we should get from surgeon's behavior is the variations of sclera force vs time whilst performing a typical surgery task like following some vessels inside the eye. By obtaining such variation, we would be able to define a maximum safe value for the sclera manipulation which would be our basis for the first Variable Admittance Control. A typical curve for this part is shown in Figure 10. In other words, our aim for how to use this plot is set at developing a Variable Admittance Control to increase the robot resistance to movement when the sclera force is approaching the upper safe limit developed from surgeon's behavior. This controller is mainly focused on increasing safety of sclera tissue.
- The second curve we should get from the surgeon's behavior is the curve of sclera force vs insertion depth. By having such figure, we would be able to define a measure of dexterous manipulation which would be our basis for the second Variable Admittance Control. Indeed, we set our aim in this part at developing another Variable Admittance Control to coerce the robot to move in such a way to make the sclera force – insertion depth curve to be similar to the previously established standard curve. A typical curve for this part from a novice subject is shown in Figure 11. In this figure, the scattered cloud which is in light blue is the aggregation of all force-depth points when the surgeon is manipulating the eyeball. The curve plotted with circle marker is the average of all sclera forces in a fixed insertion depth. Furthermore, the pink and blue curves are also the best 3rd order polynomial and the Bernstein polynomials fitted to that circled curve, respectively. In contrary to the previous standard which was intended to handle the safety, this one would be focused on increasing the dexterity in manipulating the eye.

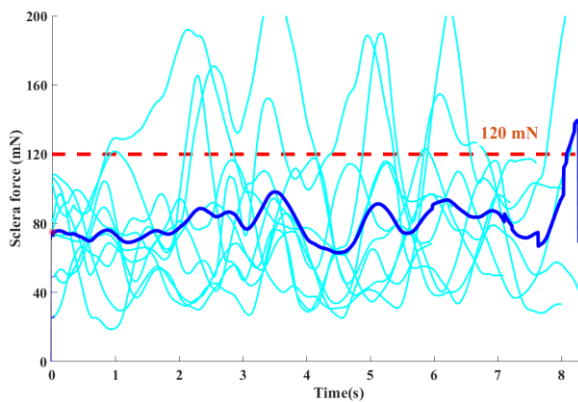


Figure 10: Maximum sclera force information from a surgeon's behavior is defined to be 120 mN

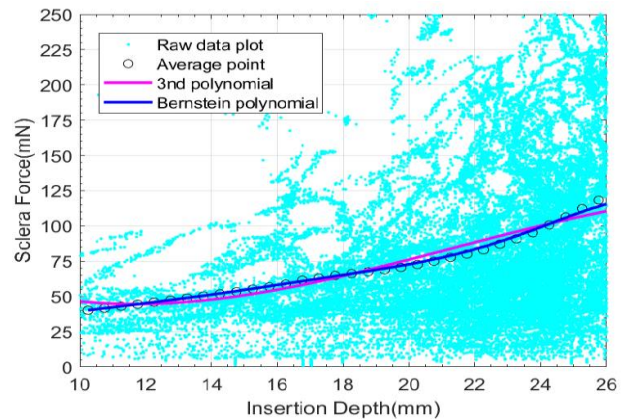


Figure 11: Sclera force vs insertion depth in a typical eye-surgery task (for a novice operator)

3.3 Control approaches.

For the purpose of sclera safety, 2 different control approaches have been adopted each of which accounts for its corresponding standard developed in section 3.2 . The first control approach is essentially an exponential gain that increases the robot resistance when the sclera force as the sclera force approaches the upper safe limit of 120 mN which was defined in Figure 10. The second control approach is basically an adaptive force control which is derived from [8]. This controller tries to move the robot in a way that the sclera force will follow the desired sclera force which is defined in Figure 11. In addition, we have adopted another procedure to increase the sclera tissue safety which is providing auditory feedback to the subjects as the sclera force is reaching the detrimental levels.

Approaches number one and three were implemented on the real robot and evaluated with some subjects. Furthermore, the method number 3 was evaluated by hiring 10 users around the campus as a multi-user experiment. However, the second method which was a quite intricate method was just simulated with a 1DOF robot in SIMULINK and as a future goal we aim at implementing the controller which is working very well in the simulations on the real robot.

The general architecture for the control problem is shown in Figure 12. The user interaction force F_h and also the real sclera forces F_s are feedback to the admittance controller and then the controller produces desired velocities for robot joints to follow.

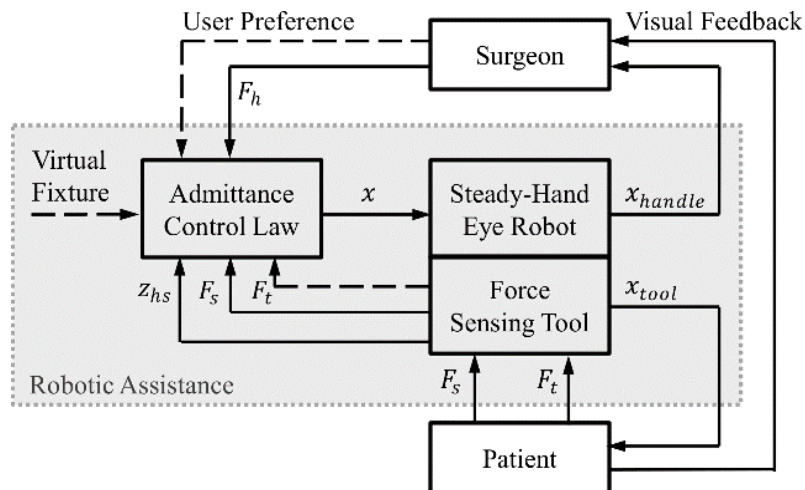


Figure 12: General control architecture

3.3.1 The first variable admittance control

As mentioned before, the purpose of this controller is to make the robot comply with the first standard safety measure attained from the surgeon's behavior. Therefore, we should

increase the robot resistance as the sclera force is approaching the unsafe upper value of 120 mN.

In order to gradually increase the robot resistance as the sclera force approaches the upper safe value of 120 mN, another variable exponential coefficient is applied to the right-hand-side of Eq. (1). This coefficient would be equal to one if the sclera force (F_s) is below a threshold F_{start} and will exponentially decrease from one and converge to zero as the sclera force increases. If we had chosen constant gain instead of the exponential one, we would have observed kind of chattering behavior because of constantly jumping from the upper gain to the lower gain when the sclera force traverses the 120 mN threshold. Thus, the new admittance control for $F_s > F_{start}$ is indicated in Eq. (2).

$$\dot{x}_d = e^{c(-F_s + F_{start})} \Delta F_h \quad (2)$$

We have tuned the exponential power coefficient (constant c in Eq. (2)) to be 0.1 by experimenting with various values for it and observing the robot behavior. After fixing this constant to 0.1, we have plotted the exponential gain for different values of starting force (F_{start}): 60, 80 and 100 mN in Fig. It is obvious that for the case of 60 mN starting point, the gain would be very close to zero when the sclera force reaches 120 mN (the upper safe limit for sclera force) and the robot will have a high resistance to movement for the sclera forces more than 120 mN. Thus, we chose F_{start} to be 60 mN to have a very high resistance to movement when the force finally reaches the upper safe limit. Aside from that, by choosing F_{start} to be 60 mN we would have a more gradual decrease in the exponential gain before the sclera force reaches the upper safe limit of 120 mN. It should be noted that the constant values in the exponential gain can be tuned for a more optimized and desirable robot manipulation.

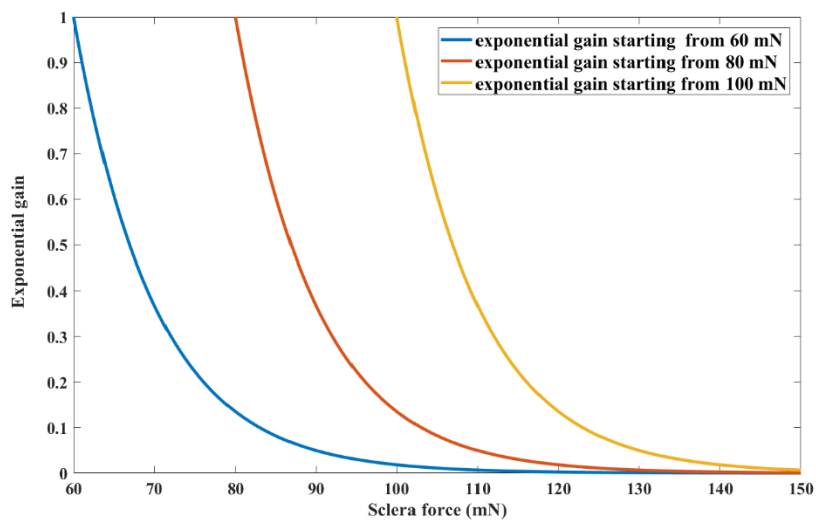


Figure 13: Exponential gain for various starting points (F_{start})

3.3.2 The second variable admittance control

The general idea for the second control is attained from the [8]. This controller tries to move the robot in a way that the sclera force will follow a desired pre-defined reference signal. If we want to explain the control in a simple way for a 1DOF system it would be as following: The polygonal mass in Figure 14 is in contact with a flexible environment with unknown flexibility γ . The mass can be assumed as a 1DOF velocity-controlled (servo control on robot velocity) robot. In other words, by defining a desired velocity for the robot (\dot{x}_d), the built-in velocity controller of the robot will try to follow that desired velocity and make the robot velocity (\dot{x}) converge to \dot{x}_d . Our purpose would be to control the mass interaction force with its environment $f_c(t)$ such as it will follow a predefined desired reference signal $f_d(t)$. In other words, we want to decide how to build the desired reference velocity signal of the robot such as the robot will follow the desired reference force signal $f_d(t)$. As it was mentioned, the environment flexibility is unknown to the robot and thus cannot be used in the control input. Roy et all [] has proved the following theorem for this problem.

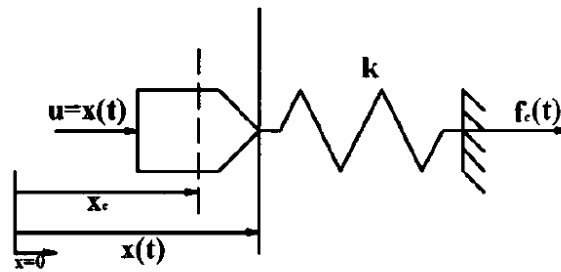


Figure 14: a simple 1DOF system to explain the control method

■ Theorem:

For any bounded C^2 reference force trajectory $f_d(t)$, with bounded time derivatives $\dot{f}_d(t)$ and $\ddot{f}_d(t)$, the control law:

$$\dot{x}_d = \hat{\gamma}(t)\dot{f}_d(t) - k_f(f_d(t) - f_c(t)) \quad (3)$$

With the adaptive update law of:

$$\dot{\hat{\gamma}}(t) = -\alpha\dot{f}_d(t)(f_d(t) - f_c(t)) \quad (4)$$

Acting on the plant:

$$\begin{aligned} \dot{x}(t) &= \dot{x}_d + \Delta\dot{x} \\ f_c(t) &= k(x(t) - x_e) \end{aligned} \quad (5)$$

Guarantee bounded force tracking error $\Delta f(t) = f_d(t) - f_c(t)$ and bounded compliance estimate $\hat{\gamma}(t)$. Further, $\Delta f(t)$ satisfies:

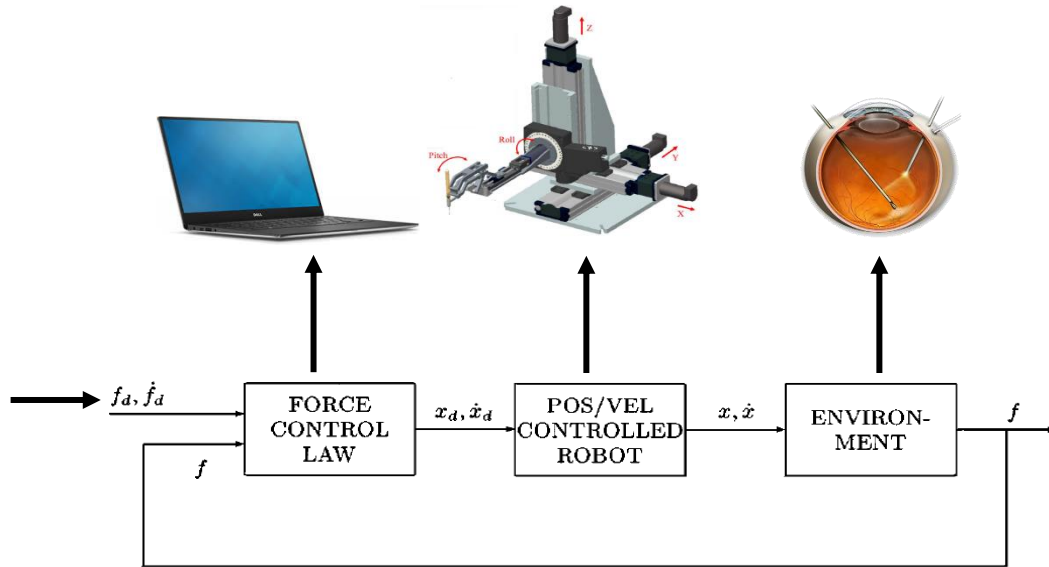


Figure 16: basic idea for the second controller

3.3.3 Auditory feedback

Audio feedback was provided to the participants for real time force monitoring. Two speakers which are connected to the computer (Figure 5) sound beeps with varying frequency depending on the measured sclera force level. To have a gradual warning about the increasing sclera force, the subjects are provided with three levels of audio feedback. The speakers sound a low-pitch low-volume noise when the sclera force passes 80 mN. This level of noise is sustained until the force reaches 100 mN; thereafter, a noise with higher frequency and medium volume is played until the sclera force approaches 120 mN. After this force level, a very high frequency tone would be emitted continuously with a high-volume.

3.4 Conclusion

As a conclusion for the technical approach part, we have applied 3 different methods to increase the sclera safety for eyeball manipulation. Beside from that, we have also assembled and programmed a piezo-actuated linear stage to simulate the movement of the eye during the surgery. In the next part, the results for these methods are presented.

4 Results

As it was mentioned before, the first and the third control approaches discussed in section 3.3 are implemented on the real robot in this project. The first and third method were assessed

using 3 subjects in different experiments without using the linear stage (pilot studies). Furthermore, we conducted multi-user experiments with 10 users using the auditory feedback method (third method) to see how it can affect enhancing the sclera safety while the eyeball position was changing during the experiments. The second method has not been implemented on the real robot yet, and one of our future goals would be implementing this method on the real robot.

4.1 Pilot studies (for the first and third control)

Four subjects including two engineers (subjects 1 and 2) and two clinicians, one beginner surgeon (subject 3) and one retinal surgeon with more than 20 years of experience (subject 4) participated in this study, and they were asked to look into the microscope and follow the colored vessels depicted in Fig. 4 while maintaining the tool tip as close as possible to the vessels without touching them. During the experiments all the sclera force, insertion depth and robot movement information were recorded. After inserting the tool into the eyeball through the sclerotomy hole, each subject went through the following steps:

1) Subject rotates the eyeball and brings the tool tip on top of the home position (Fig. 4) in the vertical view.

2) An assistant reads one random sequence of four vessel colors for the subject. (e.g. yellow, red, blue, green)

3) The subject follows the vessels with the tool tip with the order specified in step 2 without touching the vessels.

4) After following all vessels, the subject brings the eye to the home position similar to step one.

Each subject is supposed to perform the abovementioned procedure in five sets of experiment including:

1) Non-robot-assisted (Freehand) without feedback (No fb)

2) Robot-assisted without feedback

3) Freehand with audio feedback (Audio fb)

4) Robot-assisted with audio feedback

5) Robot-assisted with haptic feedback (Haptic fb – first controller in part 3.3)

Each subject is supposed to repeat each of these five sets of experiments for 10 trials with different sequence of colors.

As an example, in Figure 17 the variations of sclera force for a single trial of each set of freehand experiments for one of the subjects are shown. In Figure 18 the same plots for the robot-assisted experiments are presented.

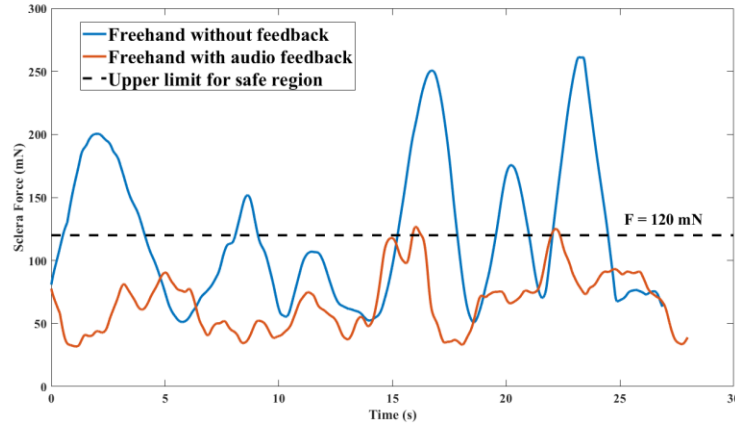


Figure 17: A trial for one set of all experiments done by one of the subjects in freehand experiments

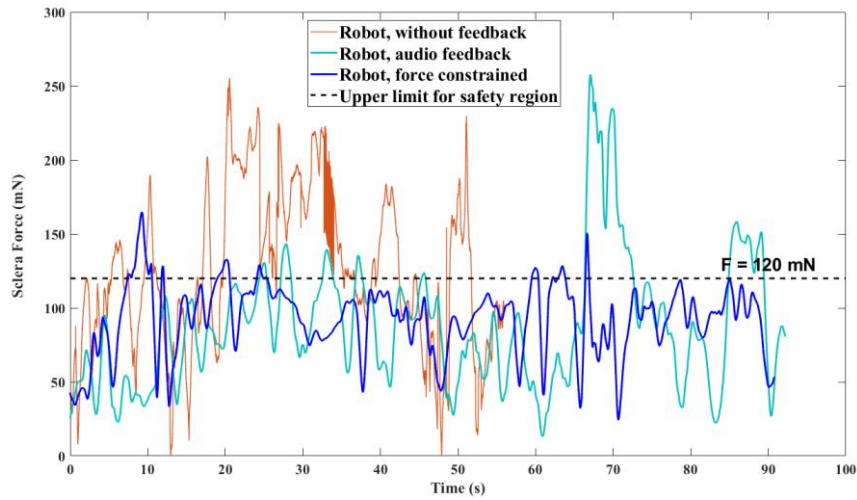


Figure 18: A trial for one set of all experiments done by one of the subjects in robot-assisted experiments

As an overall conclusion from Figure 17 and 18 which include a single trial of each experiment set, it is apparent that providing feedback has decreased the sclera force level, but the total time for those experiments have increased.

4.2 Results of the SIMULINK simulations for the second control method

As discussed before the second controller was simulated in the SIMULINK. After running the Simulink file, we would see the general picture of the 1DOF robot moving in the 1DOF eyeball which is depicted in Figure 19. The black rod is a model for 1 DOF robot and the blue circle is the eyeball. The point of application of user interaction force F_h and the sclera force represented using arrows. We set a desired sclera force of 100 mN which is changing like a sinusoidal wave changing with frequency of $w = 2$ rad/sec. The reference desired force is shown in Eq. (7).

$$f_a(t) = 0.01 \sin(2t) (N) \quad (7)$$

From Figure 20, it is observed that real sclera is following the reference sclera force after applying the adaptive controller discussed in part 3.3.2 . In another attempt, we put the desired sclera force to zero. From fig it can be seen that again the sclera force is following the reference zero signal very well. Thus, the control approach can limit the sclera force to small values very well and is working perfectly. As our future goal we want to implement the controller on the real eye-robot.

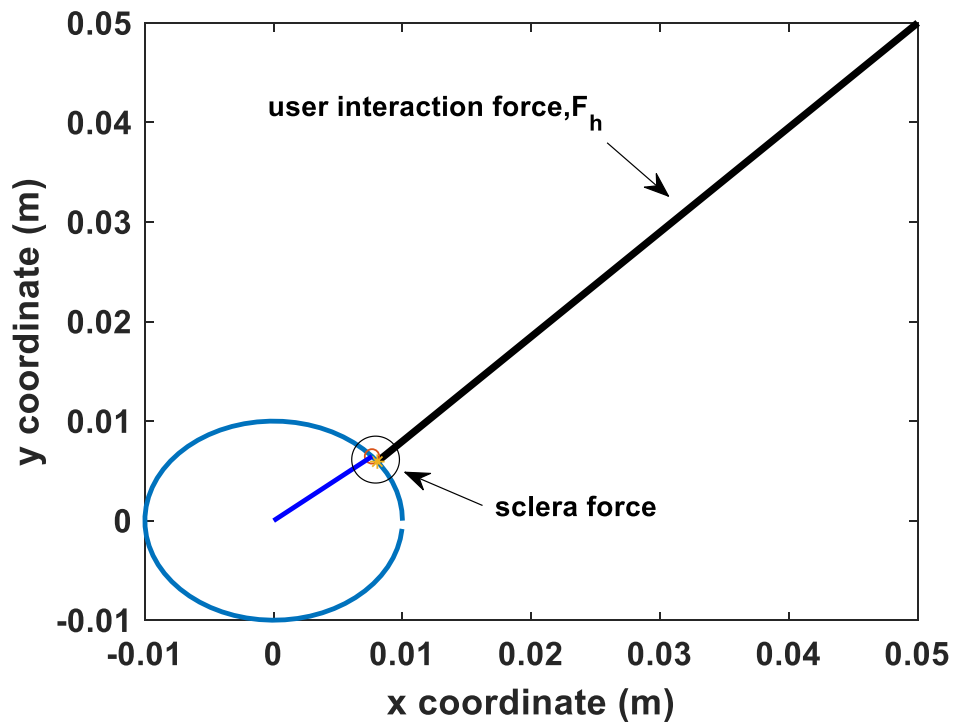


Figure 19: A screenshot of SIMULINK simulation (the black rod is a model for 1 DOF robot and the blue circle is the eyeball)

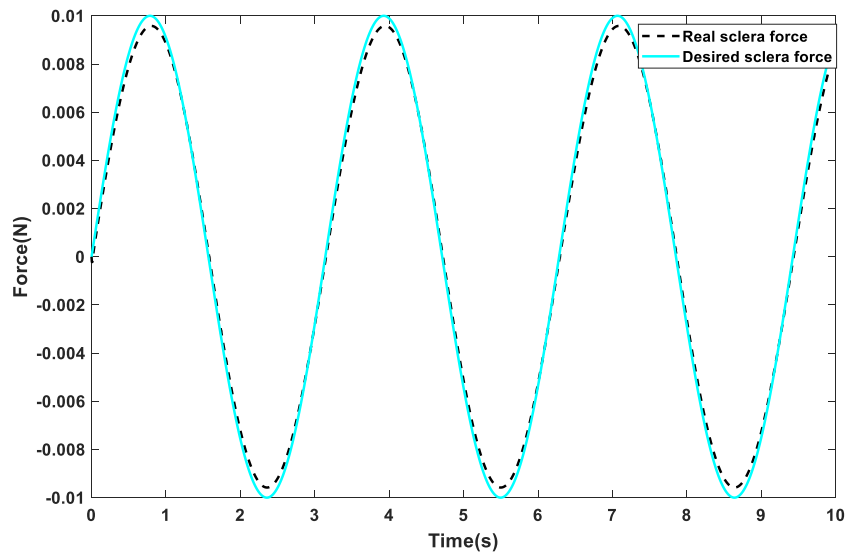


Figure 20: The plots for sinusoidal reference sclera force and the real sclera force

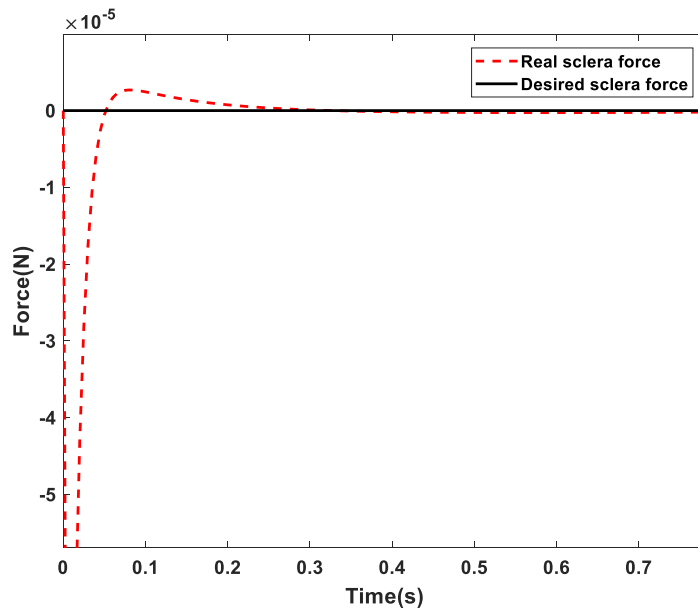


Figure 21: The plots for zero reference sclera force and the real sclera force

4.3 Multi-user experiment

For conducting the multi-user experiments, we advertised our experiment around the campus and 10 volunteers expressed their interest to take part in the experiments.

After signing the IRB consent paper, the users performed the same thing as section 4.1 except doing the following steps instead of the 5 steps mentioned in section 4.1. All the following steps included the auditory feedback.

- 1- Following 4 sequences of vessels while the stage is moving, freehand
- 2- Following 4 sequences of vessels while the stage is not moving, freehand
- 3- Following 4 sequences of vessels while the stage is moving, robot-assisted
- 4- Following 4 sequences of vessels while the stage is not moving, robot assisted

We have already finished doing the experiments with 10 users. Because the amount of data we got from the users were too much, we have just been able to analyze the data for 3 of users which is shown in Tables 1 and 2. In Tables 1 and 2, we can see the average amount of time for each user for each experiment and the ratio of the experiment time spent over forces more than 120 mN which was the unsafe limit as discussed before.

Table 1 and 2: Results of multi-user experiments for 3 of subjects

| | Robot-assisted experiments | | | |
|-----------|---|------------|---|------------|
| | <i>T = Total time elapsed average (s)</i> | | <i>Ratio of the time spent on forces more than 120 mN to the total time T</i> | |
| | Steady eye | Moving eye | Steady eye | Moving eye |
| Subject 1 | 66 | 52 | 0.11 | 0.19 |
| Subject 2 | 50 | 42 | 0.52 | 0.4 |
| Subject 3 | 50.5 | 65 | 0.16 | 0.15 |
| average | 55.5 | 53 | 0.263 | 0.247 |

| | Freehand experiments | | | |
|-----------|---|------------|---|------------|
| | <i>T = Total time elapsed average (s)</i> | | <i>Ratio of the time spent on forces more than 120 mN to the total time T</i> | |
| | Steady eye | Moving eye | Steady eye | Moving eye |
| Subject 1 | 46 | 39 | 0.12 | 0.04 |
| Subject 2 | 43 | 33 | 0.06 | 0.016 |
| Subject 3 | 48 | 40 | 0.170 | 0.014 |
| average | 45.67 | 37.33 | 0.1167 | 0.023 |

5 Conclusion

In summary, we have evaluated different approaches to increase the sclera safety for retinal surgery. The first two methods were active control approaches in which the robot tries to compensate the user's mistakes. In contrary, the third method was a passive auditory feedback in which the user just hears some beeps when the sclera force exceeds the safe thresholds. As, it was observed from the results, all three methods are appropriate in diminishing the level of sclera force and can be helpful. The most complicated method that performs the task of desired force control was the second method and one of our future steps is to implement this method on the

real robot. Also, as it can be seen from the Tables 1 and 2, it is obvious that the moving stage does not have too much effect and, the subjects have been able to sustain the sclera force in safe limits for the majority of experiment time.

6 Challenges and Issues

- 1- The first challenging part of this project was to come up with a proper force control method which would be able to make the sclera force follow a desired trajectory. As it was discussed in details, the second control approach essentially found to be able to perform this task and as observed in the results part its performance in tracking the reference sclera forces is perfect. However, as mentioned, finding the control method and customizing that control algorithm for our application was a long and hard process but finally we succeeded in implementing that control.
- 2- For the first control method, one of the main issues was to that we did not have the sclera force signal in the robot coordinate frame and thus we could not increase the robot resistance directionally because we cannot identify in which direction in the robot coordinate frame the unsafe sclera force in being exerted. The reason for that is that the tool is not rigid with respect to the robot and thus during the manipulation the tool may rotate around its shaft axis. Therefore, one of the major problems with the exponential control approach was that the robot's resistance to movement will increase in any direction and even if the subject is retracting the tool from unsafe zones. We have recently built some mechanical constraints that can be attached to the robot's wrist and will prevent the tool to rotate with respect to the robot. That will fix this problem and again one of our future goals is to bring the exponential controller some direction-based features.

7 Management Plan, Reading List and References

I shared all the files related to the project in Google Drive to ensure that I will access them anywhere and in case any emergency would happen. As far as time management, I had weekly progress meetings with my mentors and discussed the schedule and progress of the project. I had a regular weekly meeting with my mentors on Fridays in the evening. I also was in touch with mentors in case a challenging problem happened like in the control approaches. Whenever I made some progresses I used to discuss them with the mentors and get their feedback for the following steps.

8 Deliverables and Milestones

- 02/18 – Preparing the setup (Done)
- 02/28 – Deciding about the control approach by talking to the mentors (Done)

Minimum

- 03/05 - Force data accuracy and reliability (Done)
- 03/18 - Implementing the proportional VAC algorithm and tuning (Done)
- 03/28 – Doing the pilot studies to test the proportional controller (Done)

Expected

- 04/06 – Obtaining the f-d relationship for an expert surgeon (Done)
- 04/18 - Implementing the new adaptive VAC algorithm and tuning (Done)
- 04/29 – Multi-user experiments with 10 subjects using the moving stage (Done)

Maximum

- 05/10 – - Performing the experiments with clinicians (Not finished)

Thus, we have been able to finalize the main objectives of the project as discussed.

9 Acknowledgements

This project is supported by Dr. Marin Kobilarov, Dr. Iulian Iordachita, Dr. Russell H. Taylor and Dr. Nirav Patel. I would like to thank Nirav for supporting the project with programming problems. Also, I would like to thank Dr. Iordachita and Dr. Kobilarov for helping me with the scientific aspect of the project and thank Dr. Taylor for valuable general guidance.

10 References

- [1] R. Taylor, P. Jensen, L. Whitcomb, A. Barnes, R. Kumar, D. Stoianovici, P. Gupta, Z. Wang, E. DeJuan, and L. Kavoussi, "A steady-hand robotic system for microsurgical augmentation," *The International Journal of Robotics Research*, vol. 18, no. 12, pp. 1201–1210, 1999.
- [2] X. He, M. Balicki, P. Gehlbach, J. Handa, R. Taylor, and I. Iordachita, "A multi-function force sensing instrument for variable admittance robot control in retinal microsurgery," in *Robotics and Automation (ICRA), 2014 IEEE International Conference on*. IEEE, 2014, pp. 1411–1418.
- [3] *Adaptive filtering, prediction and control*, Graham C. Goodwin, Englewood Cliffs, N.J.: Prentice Hall, 2009
- [4] A. Gijbels, E. B. Vander Poorten, P. Stalmans, and D. Reynaerts, "Development and experimental validation of a force sensing needle for robotically assisted retinal vein cannulations," in *Robotics and Automation (ICRA), 2015 IEEE International Conference on*. IEEE, 2015, pp. 2270–2276.

- [5] J. T. Wilson, M. J. Gerber, S. W. Prince, C.-W. Chen, S. D. Schwartz, J.-P. Hubschman, and T.-C. Tsao, "Intraocular robotic interventional surgical system (iriss): Mechanical design, evaluation, and master–slave manipulation," *The International Journal of Medical Robotics and Computer Assisted Surgery*, 2017.
- [6] K. Willekens, A. Gijbels, L. Schoevaerdts, L. Esteveny, T. Janssens, B. Jonckx, J. H. Feyen, C. Meers, D. Reynaerts, E. Vander Poorten et al., "Robot-assisted retinal vein cannulation in an in vivo porcine retinal vein occlusion model," *Acta ophthalmologica*, vol. 95, no. 3, pp. 270–275, 2017.
- [7] S. Tanaka, K. Harada, Y. Ida, K. Tomita, I. Kato, F. Arai, T. Ueta, Y. Noda, N. Sugita, and M. Mitsuishi, "Quantitative assessment of manual and robotic microcannulation for eye surgery using new eye model," *The International Journal of Medical Robotics and Computer Assisted Surgery*, vol. 11, no. 2, pp. 210–217, 2015.
- [8] Roy, Jaydeep, and Louis L. Whitcomb. "Adaptive force control of position/velocity-controlled robots: theory and experiment." *IEEE Transactions on Robotics and Automation* 18, no. 2 (2002): 121-137.